Etching Characteristics of $YMnO_3$ Thin Films in Cl Based Inductively Coupled Plasma

Dong-Pyo Kim* and Chang-Il Kim
School of Electrical and Electronics Engineering, Chung-Ang University, 221, Huksuk-dong, Dongjak-gu, Seoul 156-756, Korea

*E-mail: dpkim@ms.cau.ac.kr

(Received 10 February 2003, Accepted 20 March 2003)

Ferroelectric $YMnO_3$ thin films were etched with Ar/Cl_2 and CF_4/Cl_2 plasma. The maximum etch rate of $YMnO_3$ thin film was 300 Å/min at a Cl_2/Ar gas mixing ratio of 8/2, an RF power of 800 W, a dc bias of –200 V, a chamber pressure of 15 mTorr, and a substrate temperature of 30 ºC. From the X-ray photoelectron spectroscopy (XPS) analysis, yttrium was not only etched by chemical reactions with Cl atoms, but also assisted by Ar ion bombardments in Ar/Cl_2 plasma. In CF_4/Cl_2 plasma, yttrium formed nonvolatile YF_x compounds and remained on and the etched surface of $YMnO_3$. Manganese etched effectively by forming volatile $MnCl_x$ and MnF_y. From the X-ray diffraction (XRD) analysis, the (0004) diffraction peak intensity of the $YMnO_3$ thin film etched in Ar/Cl_2 plasma shows lower than that in CF_4/Cl_2 plasma. It indicates that the crystallinty of the $YMnO_3$ thin film is more easily damaged by the Ar ion bombardment than the changes of stoichiometry due to nonvolatile etch by-products.

Keywords : $YMnO_3$, Inductively coupled plasma, XPS, XRD

1. INTRODUCTION

High-integrated ferroelectric random access memories (FRAMs) have been attracted many attentions due to their wide range of applications including smart cards, mobile equipments such as cellular phone, and next generation embedded memory devices. FRAMs are classified into two types; destructive readout (DRO) and nondestructive readout (NDRO)[1]. NDRO metal-ferroelectric-semiconductor field-effect transistors (MFS-FETs) have advantages due to their small cell size and simple structure. For the MFSFET structure, ferroelectric thin films must have a relatively low permittivity and a small interface state between Si and ferroelectric films[2,3]. Thus, ferroelectric $YMnO_3$ thin film is a predominant dielectric material for MFSFET structure because it has a relatively low permittivity (ε_r=20) and does not include volatile materials such as Pb and Bi which easily diffuse into the Si substrate and lead to point defects[4].

Although a lot of papers have been presented on the growth of ferroelectric $YMnO_3$ thin films[5-7], there has been little study on patterning of $YMnO_3$ films for high-integrated FRAMs. To fabricate high-integrated FRAMs, plasma etching in highly density plasma is indispensable for anisotropic pattern definition because it has good selectivity and excellent process control. However, plasma induced damage deteriorates the properties of ferroelectric thin films. Plasma induced damage classified as plasma-caused species permeation, residue contamination, bonding disruption and current flow damage [8]. Above all, the change of crystallinty and stoichiometry caused by physical ion impacts or chemical reactions seriously deteriorates the electrical properties of ferroelectirc thin films.

In this study, $YMnO_3$ films were etched with an inductively couple plasma (ICP). In order to study the etch characteristics and plasma induced damages of $YMnO_3$ thin films, we compare the etching rate of $YMnO_3$ films with adding CF_4 and Ar to Cl_2 plasma. The diagnostics of the plasma were conducted using optical emission spectroscopy (OES). The chemical states on the etched surface of $YMnO_3$ thin films were investigated with using X-ray photoelectron spectroscopy (XPS). For investigation of plasma etching damages of $YMnO_3$ film, the crystallinity and surface roughness were examined with using X-ray diffraction (XRD) and atomic force microscope (AFM).

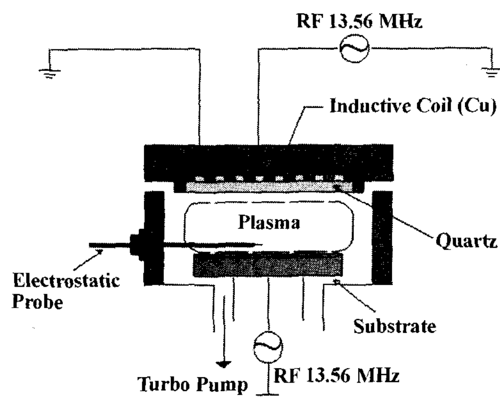

Fig. 1. Schematic illustration of the inductively coupled plasma (ICP) system.

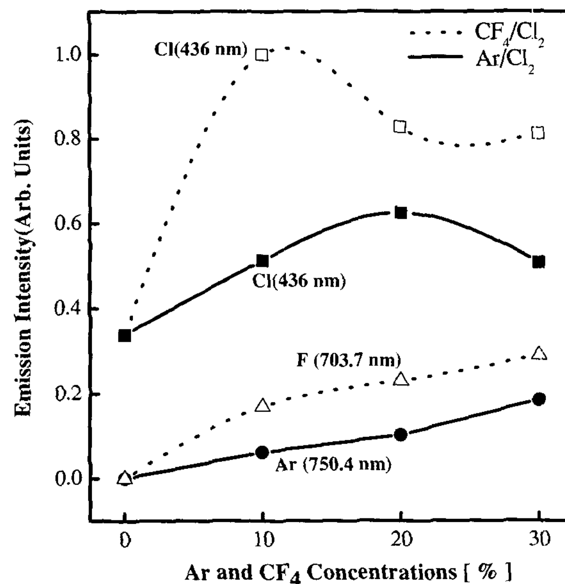

Fig. 2. Optical emission intensities of Cl, F, and Ar as a function of additive gas (Ar and CF_4) concentrations in Cl_2 plasma (coil rf power of 800 W, dc bias of –200 V and chamber pressure of 15 mTorr).

2. EXPERIMENTAL

$YMnO_3$ thin film was grown by using sol-gel method. The $YMnO_3$ coating solution was spun-coated on $Pt/Ti/SiO_2/Si$ substrates. To remove solvents, the heat treatments were performed on the hot plate at 450 °C for 10 min. The coating and heat treatment were repeated 7 times to obtain a final thickness of 3000 Å. The prepared $YMnO_3$ thin films were annealed at 850 °C in O_2 ambient for 1 h for preferred c-axis crystallization.

A schematic illustration of ICP system is shown in Fig. 1. The ICP etching equipment has a 3.5 turn copper coil on top of the chamber separated by a 24-mm-thick quartz window. To generate inductively coupled plasma, the copper coil was powered by a 13.56 MHz source. The bottom electrode was powered by a 13.56 MHz source to generate self-bias voltage.

To investigate the effects of additive gases (Ar and CF_4) in Cl_2 plasma, we etched $YMnO_3$ films with Ar/Cl_2 and CF_4/Cl_2 plasma. For these experiments, the rf power, the dc bias voltage, the chamber pressure, and the substrate temperature were fixed at 800 W, -200 V, 15 mTorr, and 30℃, respectively. The etch rates of $YMnO_3$ thin films were measured using an α-step surface profiler (KLA TENCOR). Before etching the $YMnO_3$ thin films, OES (NANOTEC NTSU-101) was used to analyze the volume densities of atoms (Cl and F) and ion (Ar) as functions of additive gas mixing ratio in Cl_2 plasmas. The relative atomic percentages and chemical reactions on the surface of the etched $YMnO_3$ films were investigated with using XPS (ESCA-LAB 220-IXL). The XPS Al-K_α source provides chromatic X-ray of 1486.6 eV. The crystallinities of the etched samples were investigated by using XRD (Rigaku-D/MAX diffractometer with CuK_α emission). The surface morphologies of $YMnO_3$ were investigated with AFM (PSI, Autoprobe CP)

3. RESULTS AND DISCUSSION

To understand the effect of additive gases (Ar and CF_4) into Cl_2 plasma, we measured the changes of active etching species with OES. Figure 2 shows the optical emission intensities of Cl (436 nm), F(703.7 nm), and Ar (750.4 nm) as a function of Ar or CF_4 mixing ratio in Cl_2 plasma. In Ar/Cl_2 plasma, the optical emission intensity of Cl increased with increasing of Ar concentration up to 20 %. The increase of the Cl atom intensity is due to the transparency effect by metastable Ar atoms. As the Ar concentration increase over 20 %, the intensity of Cl atom decreased due to the reduction of Cl_2 molecules. In CF_4/Cl_2 plasma, the optical emission intensities of the F and Cl atom increase rapidly as the CF_4 concentration increases. The optical emission intensities of the Cl have a maximum value at 10 % CF_4 concentration. This result can be explained by the fact that the addition of a small amount of CF_4 to Cl_2 enhances the generation of Cl by the reactions of following equations[9];

$$Cl_2 + F \rightarrow FCl + Cl \quad (1)$$

$$Cl_2 + CF_2 \rightarrow CClF_2 + Cl \quad (2)$$

Figure 3 shows the etch rate of $YMnO_3$ as a function of Ar and CF_4 concentration to Cl_2 plasma.

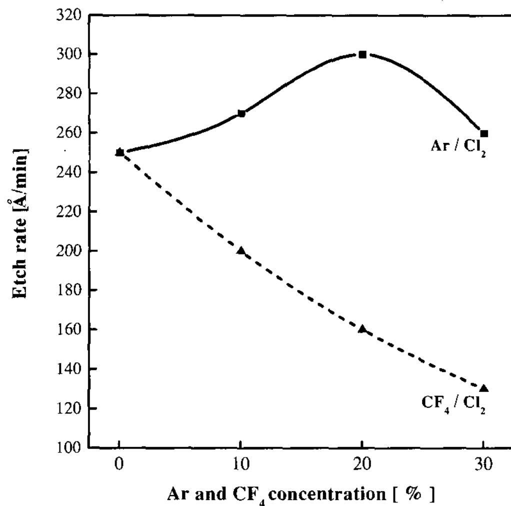

Fig. 3. Etch rate of $YMnO_3$ as a function of additive gas (Ar and CF_4) concentrations in Cl_2 plasma (coil rf power of 800 W, dc bias of –200 V and chamber pressure of 15 mTorr).

Table 1. The relative atomic percentages of $YMnO_3$ thin films for as deposited and etched with Cl_2/Ar and Cl_2/CF_4 plasma (coil rf power of 800 W, dc bias of –200 V and chamber pressure of 15 mTorr).

	Y	Mn	O	Cl	F
As-depo.	31.4	23.3	36.8		
Ar(20%)/ Cl_2(80%)	13.8	7.0	22.1	44	
CF_4(10%)/ Cl_2(90%)	25.8	5.26	27	9	16

The maximum etch rate of $YMnO_3$ film is 300 Å/min at an Ar /Cl_2 gas mixing ratio of 2/8. The etch rate of $YMnO_3$ thin film increases as the Ar concentration increases up to 20 %, and then decreases with further increase of the Ar concentration. These results indicate that $YMnO_3$ film is effectively etched by chemical reactions with Cl atoms, which was dissociated by metastable Ar ions, and physical ion bombardments of Ar. However, as the CF_4 concentration increases, the etch rate of $YMnO_3$ decreases in spite of increase of Cl. This can be explained by the fact that the accumulation of YF_x prevents from forming volatile etch byproducts.

The chemical states of $YMnO_3$ surface were investigated with XPS. The components of $YMnO_3$ (Y, Mn, and O), C, Cl and F were observed. Table 1 shows the relative atomic percentages of as-deposited $YMnO_3$ thin film and $YMnO_3$ films etched with Ar(20%)/ Cl_2(80%) and CF_4(10%)/Cl_2(90%). As shown in Table 1, the relative atomic percentages of Y and O have lowest values of 13.8 % and 22.1 % at Ar(20%) /Cl_2(80%). This indicates that metals (Y and Mn) react with Cl effectively in Ar/Cl_2 chemistry, formed metal-chlorines and they are removed from $YMnO_3$ film surface assisted by Ar ion bombardments. As CF_4 adds to Cl_2 plasma increases, the relative atomic percentage of Y and O increases but that of Cl on the surfaces of etched $YMnO_3$ decrease. As described in Fig. 2, the 10 % addition of

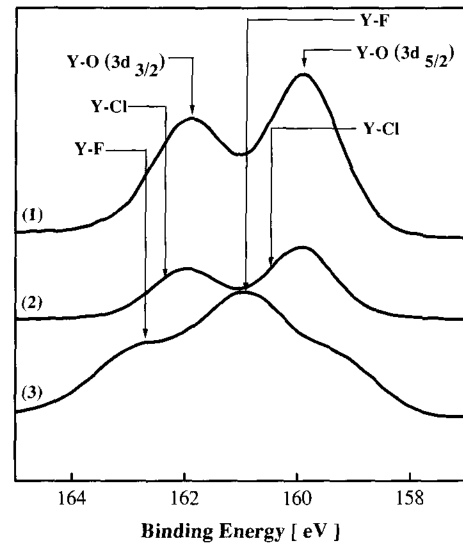

(a)

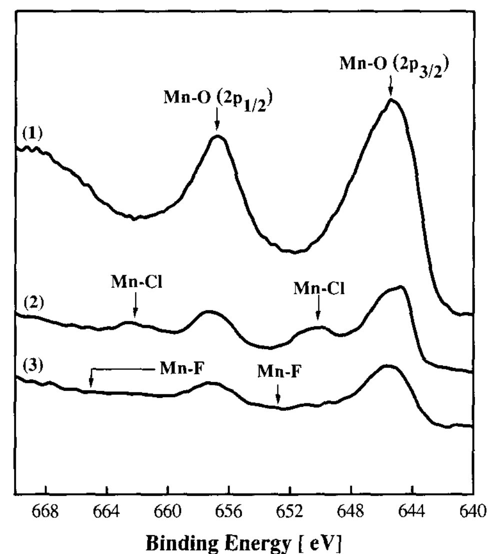

(b)

Fig. 4. (a) Y 3d and (b) Mn 2p XPS narrow-scan spectra of $YMnO_3$ thin films of (1) as deposited and $YMnO_3$ thin films etched with (2) Ar/Cl_2 and (3) CF_4/Cl_2 plasma (coil rf power of 800 W, dc bias of –200 V and chamber pressure of 15 mTorr).

CF_4 to Cl_2 plasma increases the Cl atoms; however, Y were not sufficiently reacted with Cl atoms since Y were dominantly reacted with F atoms. The electronegativity of fluorine (3.98) is higher than that of chlorine (3.0). The strength of the chemical the bonds of Y-F is stronger than that of Y-Cl[10]. Therefore, it seems that fluorine yttrium is more chemically stable than chlorine yttrium. It is more difficult to remove YF_x compounds from surface of $YMnO_3$ than YCl_x compounds because the melting points of YF_x compounds (YF_3: 1155 °C) are higher than those of YCl_x (YCl_3: 721 °C) [10]. Therefore, the YF_x compounds remains on the surfaces of $YMnO_3$ etched with CF_4/Cl_2 plasma. The relative atomic percentage of Mn is lowest at CF_4 (10%)/Cl_2(90%). This means that Mn is etched effectively by chemical reactions with Cl and F.

In order to investigate the chemical reactions between Cl and F atoms with elements of $YMnO_3$ (Y and Mn), XPS narrow scan analysis was performed. Figure 4 shows XPS narrow scan spectra of (1) as-deposited $YMnO_3$ thin film and etched $YMnO_3$ thin films at (2) an Ar(20%)/Cl_2 (80%) and (3) CF_4(10%)/Cl_2 (90%).

Figure 4(a) presents Y 3d narrow scan spectra. The peaks at 159.9 and 161.95 eV binding energies in spectrum (1) of Fig. 4(a) could be assigned to Y-O $3d_{5/2}$ and Y-O $3d_{3/2}$ bonds, respectively. As shown in spectrum (2) of Fig. 4(a) after expoed in Ar/Cl_2 plasma, the peak intensities of Y-O bonds have the lowest value. These results can be explained that the Y-O bonds are broken easily by chemical reactions between Y and Cl, and YCl_x compounds effectively removed from surface of $YMnO_3$ by Ar ion bombardments. In spectrum (3) of Fig. 4(a) after exposed in CF_4/Cl_2 plasma, the peaks at 160.9 and 162.95 eV could be assigned to Y-F bonds. As described in relative atomic percentage section, the binding energy of Y-F bond is higher than that of Y-Cl bond and the peak intensities Y-F bonds are larger than those of Y-O bonds. These results suggest that F s easily react with Y, and nonvolatile YF_x compounds remained on the etched surface due to their high melting points.

Figure 4(b) shows the Mn 2p XPS narrow scan spectra. In spectrum (1) from as-deposited films, the peaks at 645.2 eV and 656.9 eV binding energies are assigned to Mn $2p_{3/2}$–O and Mn $2p_{1/2}$–O bonds, respectively. After exposed in Ar/Cl_2 plasma (spectrum (2) of Fig. 4(b)), the peak intensities of Mn-O bonds are reduced and the new paeks are appeared at 650.2 and 661.9 eV, which could be assigned to Mn-Cl bonds. These results suggest that Mn-O bonds are broken by chemical reactions between Mn and Cl s, and then $MnCl_x$ compounds removed from $YMnO_3$ surfaces assisted by Ar ion bombardments. After exposed in CF_4/Cl_2 chemistry (spectrum (3) of Fig. 4(b)), the peaks can be resolved into three elements such as Mn-O, Mn-Cl, and Mn-F peaks[11,12]. Although we expect there will be peaks of Mn-F bonds, it is difficult to find precise binding energies of Mn-F bonds in spectrum (3) of Fig. 4(b). Thus, we can expect that there will be Mn-F peaks at higher binding energies than Mn-O and Mn-Cl peaks. As shown in Fig. 4(b), Mn-Cl bonds are reduced in CF_4/Cl_2 chemistry. Compared spectrum (3) Fig. 4(b) with Table 1, it is confirmed that F and Cl break the Mn-O bonds effectively by chemical reactions between active atoms (F and Cl) and Mn.

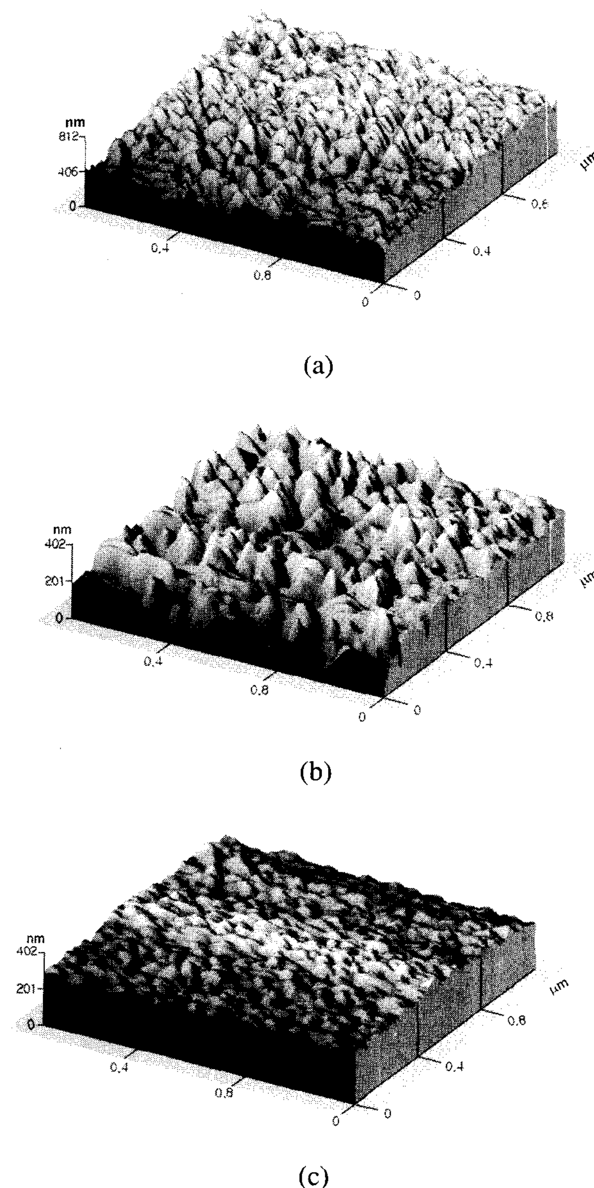

Fig. 5. AFM image of $YMnO_3$ thin films;(a) As deposited (b) etched with Ar/Cl_2 plasma, and (c) etched with CF_4/Cl_2 plasma (coil rf power of 800 W, dc bias of –200 V and chamber pressure of 15 mTorr).

Figure 5 show the surface morphologies of $YMnO_3$ for (a) as-deposited and etched As shown in Fig. 5(a), grains of as-deposited $YMnO_3$ thin film are well developed and the root mean square (rms) roughness is 4.4 nm. The rms surface roughness of the $YMnO_3$ at an Ar/Cl_2 plasma is 5.7 nm. This can be explained by the fact that elements of $YmnO_3$ and etch byproducts could be etched different ways due to Ar bombardment. The surface roughness of $YMnO_3$ thin film has a largest rms value at the Ar/Cl_2 chemistry. However, rms at CF_4/Cl_2 plasma is 3.1 nm. In CF_4/Cl_2 chemistry, the surface roughness of $YMnO_3$ thin film decreased compared with as-deposited sample because etching by-product (such as Y-F) remained on the surface of the $YMnO_3$ film due to their high melting points.

Figure 6 shows XRD patterns of $YMnO_3$ thin film for (a) as-deposited, etched with (b) $Ar(20\%)/Cl_2(80\%)$ and (c) $CF_4(10\%)/Cl_2(90\%)$. As shown Fig. 6, an as-deposited $YMnO_3$ thin film showed a good crystallization to preferred c-axis orientation, but any secondary phases were not observed. After etched with Ar/Cl_2 plasma, the peak intensity of (0004) of the $YMnO_3$ thin is much lower than that of as-deposited $YMnO_3$ film. However, the peak intensity of (0004) of $YMnO_3$ thin film etched with CF_4/Cl_2 plasma decreases a little. From these results, it is assumed that the hexagonal crystalline of $YMnO_3$ thin film is more easily damaged by Ar ion bombardments than changes of stoichiometry on the film surface due to non-volatility of the etch by products.

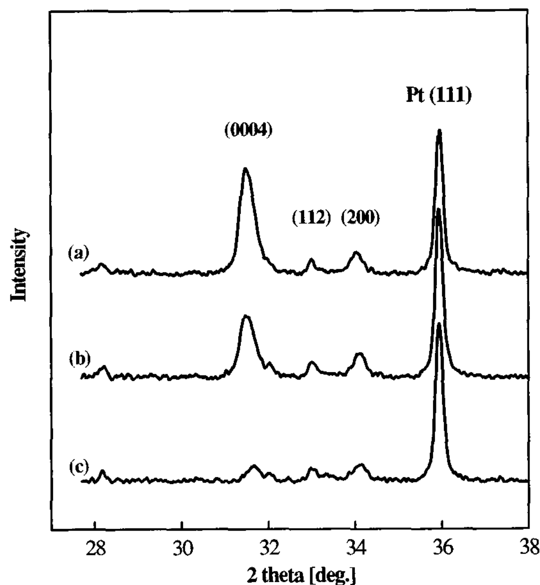

Fig. 6. XRD patterns of $YMnO_3$ thin films of (a) as deposited and $YMnO_3$ thin films etched with (b) Cl_2/Ar and (c) Cl_2/CF_4 plasma (coil rf power of 800 W, dc bias of –200 V and chamber pressure of 15 mTorr).

4. CONCLUSION

In this work, $YMnO_3$ thin films were etched with Ar/Cl_2 and CF_4/Cl_2 inductively coupled plasma. The maximum etch rate of $YMnO_3$ thin films was 300 Å/min at an Ar $/Cl_2$ gas mixing ratio of 2/8, an rf power of 800 W, a dc bias voltage of –200 V, a chamber pressure of 15 mTorr, and a substrate temperature of 30 °C. Addition of Ar to Cl_2 caused $YMnO_3$ etch rate to increase. In contrast, addition of CF_4 to Cl_2 caused $YmnO_3$ etch rate to decrease. From XPS analysis, Y and Mn react with Cl s effectively with Ar/Cl_2 plasma, and they are removed from $YMnO_3$ film surface assisted by Ar ion bombardments. However, the addition of CF_4 forms the nonvolatile fluoride yttrium remained on the etched surfaces. From AFM and XRD analyses, the $YMnO_3$ thin film etched with Ar/Cl_2 plasma was more damaged than $YMnO_3$ thin film etched with CF_4/Cl_2 plasma. Thus, it is assumed that the damage of $YMnO_3$ film by Ar ion bombardments during etch process is more severe than damage of $YMnO_3$ film caused by changes of stoichiometry on the film surface due to nonvolatile etch by products.

REFERENCES

[1] T. Toshimura, N. Fujimura, and D. Ito, "Characterization of ferroelectricity in metal/ferroelectric/insulator/semiconductor structure by pulsed C–V measurement; ferroelectricity in $YMnO_3/Y_2O_3/Si$ structure", J. Appl. Phys., Vol. 87, p. 3444, 2000.

[2] M. Alexe, G. Kastner, D. Hesse, and U. Gosele, "Ferroelectric-semiconductor heterostructures obtaned by direct wafer bonding", Appl. Phys. Lett., Vol. 70, p. 3416, 1997.

[3] D. Mou, C. S. Petterson, J. Linnros, and K. V. Rao, "Fabrication and properties of metal/ferroelectrics/semiconductor diodes on 4H–SiC", Appl. Phys. Lett., Vol. 73, p. 1532, 1998.

[4] S. Imada, T. Kuraoka, E. Tokumitsu, and H. Ishiwara, "Ferroelectricity of $YMnO_3$ thin films on $Pt(111)/Al_2O_3(0001)$ and $Pt(111)/Y_2O_3(111)/Si(111)$ structures grown by molecular beam epitaxy", Jpn. J. Appl. Phys., Vol. 40, p. 666, 2001.

[5] H. N. Lee, Y. T. Kim, and Y. K. Park, "Memory window of highly c-axis oriented ferroelectric $YMnO_3$ thin films", Appl. Phys. Lett., Vol. 74, p. 3887, 1999.

[6] H. Kitahara, K. Tadanaga, T. Minami, N. Fujiura, and T. Ito, "Lowering the crystallization temperature of $YMnO_3$ thin films by the Sol-Gel method using an yttrium alkoxide", Jpn. J. Appl. Phys., Vol. 38, p.5448, 1999.

[7] J. Y. Kim, B. K. Kim, K. E. Kim, S. T. Chung, and

S. H. Cho, "Sintering and dielectric properties of $YMnO_3$ ceramics with the effect of Y/Mn ratio", J. of KIEEME (in Korean), Vol. 13, p.137 (2000)
[8] T. Shibano, T. Takenaga, K. Nakamura, and T. Oomori, "Etching of $(Ba,Sr)TiO_3$ film by chlorine plasma", J. Vac. Sci. Tech. A, Vol. 18, p. 2080, 2000.
[9] J. K. Jung and W. J. Lee, "Dry etching characteristics of $Pb(Zr,Ti)O_3$ films in CF_4 and Cl_2/CF_4 inductively coupled plasmas", Jpn. J. Appl. Phys., Vol. 40, p. 1408 , 2001.
[10] "Handbook of Chemistry and Physics", edited by D. R. Lide, CRC Press, 1998.
[11] B. J. Min, E. G. Chang, and C. I. Kim, "Dry etching characteristics of $YMnO_3$ thin films using inductively coupled plasma", J. of KIEEME (in Korean), Vol. 14, p.93 (2001)
[12] D. P. Kim, C. I. Kim, and C. I. Lee, "Etching mechanism of $YMnO_3$ thin films in high density CF_4/Ar plasma", J. of KIEEME (in Korean), Vol. 14, p.959, 2001.